

# Blockade of the CD47/SIRP $\alpha$ checkpoint axis potentiates the macrophage-mediated antitumor efficacy of tafasitamab

Alexander Biedermann,<sup>1</sup> Maria Patra-Kneuer,<sup>2</sup> Dimitrios Mougiakakos,<sup>3</sup> Maike Büttner-Herold,<sup>4</sup> Doris Mangelberger-Eberl,<sup>2</sup> Johannes Berges,<sup>1</sup> Christian Kellner,<sup>5</sup> Sarah Altmeyer,<sup>6</sup> Jörg Thomas Bittenbring,<sup>6</sup> Christian Augsburg,<sup>2</sup> Kristina Ilieva-Babinsky,<sup>2</sup> Stefan Haskamp,<sup>7</sup> Fabian Beier,<sup>8</sup> Christopher Lischer,<sup>9</sup> Julio Vera,<sup>9</sup> Anja Lührmann,<sup>10</sup> Simone Bertz,<sup>11</sup> Simon Völkl,<sup>1</sup> Benedikt Jacobs,<sup>1</sup> Stefan Steidl,<sup>2</sup> Andreas Mackensen<sup>1</sup> and Heiko Bruns<sup>1</sup>

<sup>1</sup>Department of Internal Medicine 5, Hematology and Oncology, Friedrich-Alexander-University Erlangen-Nürnberg, Erlangen; <sup>2</sup>Translational Research, MorphoSys AG, Planegg; <sup>3</sup>Department of Hematology and Oncology, Otto-von-Guericke University (OVGU) Magdeburg, Magdeburg; <sup>4</sup>Department of Nephropathology, Institute of Pathology, Friedrich-Alexander-University Erlangen-Nürnberg (FAU), Erlangen; <sup>5</sup>Division of Transfusion Medicine, Cell Therapeutics and Hemastaseology, University Hospital, LMU Munich, Munich; <sup>6</sup>Medizinische Klinik I, Saarland University Medical School, Homburg/Saar; <sup>7</sup>Institute of Human Genetics, University Hospital Erlangen, Friedrich-Alexander-University Erlangen-Nürnberg, Erlangen; <sup>8</sup>Department of Oncology, Hematology and Stem Cell Transplantation, RWTH Medical School, Aachen; <sup>9</sup>Department of Dermatology, University Hospital Erlangen, Erlangen; <sup>10</sup>Mikrobiologisches Institut, Universitätsklinikum Erlangen, Friedrich-Alexander-Universität Erlangen-Nürnberg, Erlangen and <sup>11</sup>Institute of Pathology, Universitätsklinikum Erlangen, Friedrich-Alexander-Universität Erlangen-Nürnberg, Erlangen, Germany

**Correspondence:** H. Bruns  
heiko.bruns@uk-erlangen.de

**Received:** December 29, 2023.  
**Accepted:** June 19, 2024.  
**Early view:** June 27, 2024.

<https://doi.org/10.3324/haematol.2023.284795>

©2024 Ferrata Storti Foundation

Published under a CC BY-NC license



## Abstract

Macrophages are one of the key mediators of the therapeutic effects exerted by monoclonal antibodies, such as the anti-CD19 antibody tafasitamab, approved in combination with lenalidomide for the treatment of relapsed or refractory diffuse large B-cell lymphoma (DLBCL). However, antibody-dependent cellular phagocytosis (ADCP) in the tumor microenvironment can be counteracted by increased expression of the inhibitory receptor SIRP $\alpha$  on macrophages and its ligand, the immune checkpoint molecule CD47, on tumor cells. The aim of this study was to investigate the impact of the CD47-SIRP $\alpha$  axis on tafasitamab-mediated phagocytosis and explore the potential of anti-CD47 blockade to enhance its antitumor activity. Elevated expression of both SIRP $\alpha$  and CD47 was observed in DLBCL patient-derived lymph node biopsies compared to healthy control lymph nodes. CRISPR-mediated CD47 overexpression affected tafasitamab-mediated ADCP *in vitro* and increased expression of SIRP $\alpha$  on macrophages correlated with decreased ADCP activity of tafasitamab against DLBCL cell lines. A combination of tafasitamab and an anti-CD47 blocking antibody enhanced ADCP activity of *in vitro*-generated macrophages. Importantly, tafasitamab-mediated phagocytosis was elevated in combination with CD47 blockade using primary DLBCL cells and patient-derived lymphoma-associated macrophages in an autologous setting. Furthermore, lymphoma cells with low CD19 expression were efficiently eliminated by the combination treatment. Finally, combined treatment of tafasitamab and an anti-CD47 antibody resulted in enhanced tumor volume reduction and survival benefit in lymphoma xenograft mouse models. These findings provide evidence that CD47 blockade can enhance the phagocytic potential of tumor-targeting immunotherapies such as tafasitamab and suggest that there is value in exploring the combination in the clinic.

## Introduction

Diffuse large B-cell lymphoma (DLBCL) is the most common type of non-Hodgkin lymphoma.<sup>1</sup> Approximately 60-70% of

newly diagnosed DLBCL patients can be cured using first-line standard of care - a combination of the anti-CD20 antibody rituximab and cyclophosphamide, doxorubicin, vincristine, and prednisone (R-CHOP). The remaining 30-40% of DLBCL

patients experience relapse or refractory disease with poor survival rates. This highlights an unmet clinical need for more effective therapies for a substantial subset of patients.<sup>2,3</sup>

Tafasitamab is an Fc-modified, humanized monoclonal anti-CD19 antibody immunotherapy. Tafasitamab received accelerated approval by the Food and Drug Administration (2020) and conditional marketing authorization by the European Medicines Agency (2021) for the treatment of transplant-ineligible adult patients with relapsed or refractory DLBCL in combination with the immunomodulatory drug lenalidomide. The Fc region of tafasitamab was engineered to bind Fc $\gamma$  receptors with higher affinity than a wild-type counterpart, resulting in enhanced antibody-dependent cell-mediated cytotoxicity (ADCC)<sup>4</sup> and antibody-dependent cellular phagocytosis (ADCP).<sup>5</sup>

Macrophages are critical mediators of antibody therapy in DLBCL and represent one of the key components of the lymphoma microenvironment.<sup>6,7</sup> However, lymphoma-associated macrophages (LAM) are often compromised by the tumor microenvironment in executing their effector functions.<sup>8-10</sup> In particular, the checkpoint molecule CD47 has been shown to be highly expressed by various types of B-cell-derived lymphomas. CD47 mediates immune escape from macrophage-mediated phagocytosis upon interaction with phagocyte-expressed signal regulatory protein alpha (SIRP $\alpha$ ), a protein expressed by macrophages, granulocytes, and dendritic cells.<sup>11</sup> Furthermore, the frequency of SIRP $\alpha$ -expressing LAM was reported to be increased in patients with follicular lymphoma who relapsed after initial treatment with lenalidomide and rituximab, indicating that macrophages with reduced phagocytic capacity may influence the outcome of antibody immunotherapy regimens.<sup>12</sup> However, antibody blockade of either CD47 or SIRP $\alpha$  was shown to strongly enhance ADCP by macrophages.<sup>10,13</sup> Furthermore, a recent report of a phase Ib study suggested there may be promise in the combination of CD47 blockade with rituximab in patients with B-cell non-Hodgkin lymphoma.<sup>14</sup> Based on the reported properties of the CD47-SIRP $\alpha$  axis of interfering with innate and antibody-dependent phagocytosis, we hypothesized that combining tafasitamab with a CD47 blocking antibody could increase its ADCP activity and would have the potential to improve its efficacy.

## Methods

### Isolation of lymphoma-associated macrophages, macrophages or lymphoma cells from human samples

Bone marrow samples from healthy individuals or DLBCL patients (with pre-confirmed tumor cell infiltration), and lymph node biopsies (single cell suspension) from DLBCL patients (with pre-confirmed tumor cell infiltration) were stained with CD163, CD15 and CD20 antibodies. Macrophages (CD163<sup>+</sup>/CD15<sup>-</sup>) and B cells (CD20<sup>+</sup>) were isolated by fluorescence-activated cell sorting (FACS). Purity was greater than

95%, as determined via flow cytometry. All human material was obtained with written informed consent in accordance with the Declaration of Helsinki and its use was approved by institutional ethics committees (Aachen: EK206/09; Erlangen: ref. number 3555, 36\_12 B, 219\_14B, 200\_12B).

### Flow cytometry-based phagocytosis assay

CPD-labeled lymphoma cells were co-cultured with macrophages (effector to target cell ratio, 5:1) in sterile FACS tubes in the presence or absence of tafasitamab (1  $\mu$ g/mL) and/or anti-CD47 antibody (B6H12, 1  $\mu$ g/mL) for 24 h in R10 medium supplemented with heat-inactivated fetal calf serum (at 56°C for 30 minutes, to inactivate complement). In some experiments, the CD47-IgG $\sigma$  clone (1  $\mu$ g/mL) was used instead.<sup>15</sup> Target lymphoma cells were stained with CPD and macrophage effector cells were counterstained with anti-human CD11b-PeCy7 antibody. Absolute numbers of surviving CD11b<sup>-</sup>/CPD<sup>+</sup> lymphoma cells were determined using 123count eBeads (eBioscience). The percentage of antibody-mediated phagocytosis was calculated using the following formula: [%] = 100 - ([absolute number of surviving lymphoma cells in the presence of antibody / absolute number of surviving lymphoma cells in absence of antibody]  $\times$  100).

### Fluorescence microscopy-based phagocytosis assay

Lymphoma cells were stained with Incucyte<sup>®</sup> Cytolight Rapid Green Dye and co-cultured with macrophages (effector to target cell ratio, 1:1) on an eight-chamber slide in the presence or absence of tafasitamab (1  $\mu$ g/mL) and/or anti-CD47 antibody (B6H12, 1  $\mu$ g/mL), for 3 h. Adherent cells were washed with phosphate-buffered saline (PBS) and stained with anti-human CD11b-APC antibody and subsequently fixed with 4% paraformaldehyde in PBS. The slide was overlaid with 4',6-diamidino-2-phenylindole (DAPI) medium, covered with a glass cover slide and stored in the dark at 4°C. Slides were analyzed in z-stack sections creating up to ten optical slices (0.5  $\mu$ m thick each) using a confocal microscope (LSM700, Zeiss) at x630 magnification. To analyze phagocytosis activity, at least five different fields of view per condition and up to 100 macrophages in total were counted in a blinded manner.

### Statistical analysis

GraphPad Prism and Microsoft Excel software were used for statistical analyses. Comparisons between patients and controls were performed with a nonparametric Mann-Whitney U test. For *in vitro* experiments, a two-tailed Student *t* test was performed pairwise between treatment and control groups or between single and combination treatment groups. Results are presented as mean  $\pm$  standard error of the mean. For *in vivo* experiments, survival data were analyzed using a logrank (Mantel-Cox) test. Differences were considered statistically significant when the *P* value was <0.05.

Additional methods used in this study are described in the *Online Supplementary Methods*.

## Results

### Increased expression of CD47 and SIRP $\alpha$ in diffuse large B-cell lymphoma

Interaction of CD47 with SIRP $\alpha$  triggers a “don’t eat me” signal in macrophages, inhibiting efficient ADCP. To investigate whether the CD47-SIRP $\alpha$  axis is altered in DLBCL patients, we performed multiplex immunostaining including CD47, CD19, CD68 (a pan-macrophage marker), and SIRP $\alpha$  in specimens from patients with DLBCL (N=9) or non-malignant controls (N=7) (for the patients’ characteristics see *Online Supplementary Tables S1 and S2*). We found strongly enhanced CD47 expression on lymphoma cells compared to healthy donor B cells (mean value of the DLBCL group: 777 $\pm$ 135 mean fluorescence intensity [MFI] vs. mean value of the control group: 277 $\pm$ 58 MFI;  $P$ <0.0001) (Figure 1A, *Online Supplementary Figure S1A*). Moreover, the percentage of CD47<sup>+</sup> B cells in DLBCL specimens was also significantly increased compared to that in healthy donors (*Online Supplementary Figure S1C*). Simultaneously, SIRP $\alpha$  levels were significantly elevated on LAM of DLBCL patients (mean value of the DLBCL group: 1,824 $\pm$ 462 MFI vs. mean value of the control group: 627 $\pm$ 102 MFI;  $P$ <0.0001) in comparison to healthy donor macrophages (Figure 1B, *Online Supplementary Figure S1B*). To determine whether this observation was limited to lymph nodes or also found in the bone marrow of lymphoma patients, we examined CD47 and SIRP $\alpha$  expression in tumor-infiltrated bone marrow biopsies of DLBCL patients (N=9) using flow cytometry (for the patients’ characteristics see *Online Supplementary Table S2*) (Figure 1C, D). Similar to the pattern observed in lymph node samples, bone marrow-infiltrating lymphoma cells displayed significantly increased expression of CD47 compared to B cells in bone marrow samples from healthy individuals (N=8) (controls: 5,977 $\pm$ 3,530 MFI vs. DLBCL: 12,535 $\pm$ 3,744 MFI;  $P$ =0.002) (Figure 1C). In addition, LAM in the bone marrow of DLBCL patients showed an increased expression of SIRP $\alpha$  (controls: 8,981 $\pm$ 2,206 MFI vs. DLBCL: 12,856 $\pm$ 1,781 MFI;  $P$ =0.001) in comparison to bone marrow macrophages of healthy controls (Figure 1D). Furthermore, we used publicly available transcriptomics data (GSE178965) from lymph node biopsies of newly diagnosed or relapsed DLBCL patients to analyze CD47 and SIRP $\alpha$  expression patterns (*Online Supplementary Figure S2*). Transcriptomic analysis revealed that CD47 and SIRP $\alpha$  mRNA expression levels in relapsed patients were similar to those in newly diagnosed patients, suggesting that the CD47-SIRP $\alpha$  axis may represent a hurdle to effective antibody therapy in both relapsed and newly diagnosed DLBCL patients.

### The CD47-SIRP $\alpha$ axis impairs tafasitamab-mediated phagocytosis

Based on the elevated expression of CD47 and SIRP $\alpha$  in DLBCL, we reasoned that the “don’t eat me” axis could affect tafasitamab-mediated phagocytosis. To test this,

we performed a flow cytometric phagocytosis assay<sup>16</sup> using macrophages with variable levels of SIRP $\alpha$  expression as effector cells and different DLBCL cell lines (HT, Toledo, U2946) as target cells. CD19 and CD47 expression were in a similar range in the tested cell lines (*Online Supplementary Figure S3*). Interestingly, we discovered a significant inverse correlation between the level of SIRP $\alpha$  expression (determined as SIRP $\alpha$  MFI) and tafasitamab-mediated phagocytosis (HT: coefficient = 0.39,  $P$ =0.017; Toledo: coefficient = 0.75,  $P$ <0.001; U2946: coefficient = 0.56,  $P$ =0.002) (Figure 2A), suggesting that high SIRP $\alpha$  expression on macrophages can attenuate tafasitamab’s phagocytic potential *in vitro*. Next, we examined the effects of differential CD47 expression on tafasitamab-mediated phagocytosis. Using CRISPR/Cas9 genome editing, we generated a CD47 knockout variant (CD47<sup>KO</sup>) and a CD47-overexpressing variant (CD47<sup>high</sup>) from the wild-type (WT) Toledo cell line. While CD47 was barely detectable by flow cytometry, on CD47<sup>KO</sup> cells, CD47<sup>high</sup> cells showed a 2-fold increase compared to wild-type cells (Figure 2B). Macrophages were co-incubated with the different variants in the presence or absence of tafasitamab and phagocytosis was measured by flow cytometry. Compared to the wild-type cells, the CD47 knockout variant was increasingly phagocytosed by macrophages, whereas the CD47-overexpressing cells were resistant to tafasitamab-mediated phagocytosis (WT: 31 $\pm$ 6%; CD47<sup>KO</sup>: 55 $\pm$ 5%; CD47<sup>high</sup>: 7 $\pm$ 4%) (Figure 2C). To confirm this result, we analyzed tafasitamab-mediated uptake of the Toledo variants by confocal microscopy. After incubation for 3 h, tafasitamab induced a nearly complete uptake of all observable CD47<sup>KO</sup> cells, whereas most CD47<sup>high</sup> lymphoma cells were not phagocytosed (Figure 2D, E). Overall, these data suggest that elevated expression of both CD47 on lymphoma cells and SIRP $\alpha$  on macrophages may negatively influence the ADCP activity of tafasitamab.

### Blocking CD47 increases tafasitamab-mediated phagocytosis

Next, we aimed to counteract the effects of the CD47-SIRP $\alpha$ -axis by using an anti-CD47 monoclonal antibody. For this purpose, we analyzed phagocytosis of lymphoma cells upon combined treatment of tafasitamab and an anti-CD47 monoclonal antibody (clone: B6H12). Using confocal microscopy, we observed that the combination resulted in significantly increased phagocytosis of all tested cell lines, compared to the phagocytosis with single treatments (Figure 3A, *Online Supplementary Figure S4*). This result was confirmed in flow cytometric phagocytosis assays, demonstrating that combined treatment with tafasitamab and anti-CD47 monoclonal antibody significantly increased phagocytosis rates (%) of Toledo (tafasitamab: 32 $\pm$ 24% vs. tafasitamab + anti-CD47: 72 $\pm$ 21%;  $P$ <0.001), U2946 (tafasitamab: 32 $\pm$ 18% vs. tafasitamab + anti-CD47: 72 $\pm$ 19%;  $P$ =0.002), and HT (tafasitamab: 32 $\pm$ 17% vs. tafasitamab + anti-CD47: 72 $\pm$ 16%;  $P$ <0.001) cells (Figure 3B). Since the previous experiments represent only a snapshot at the

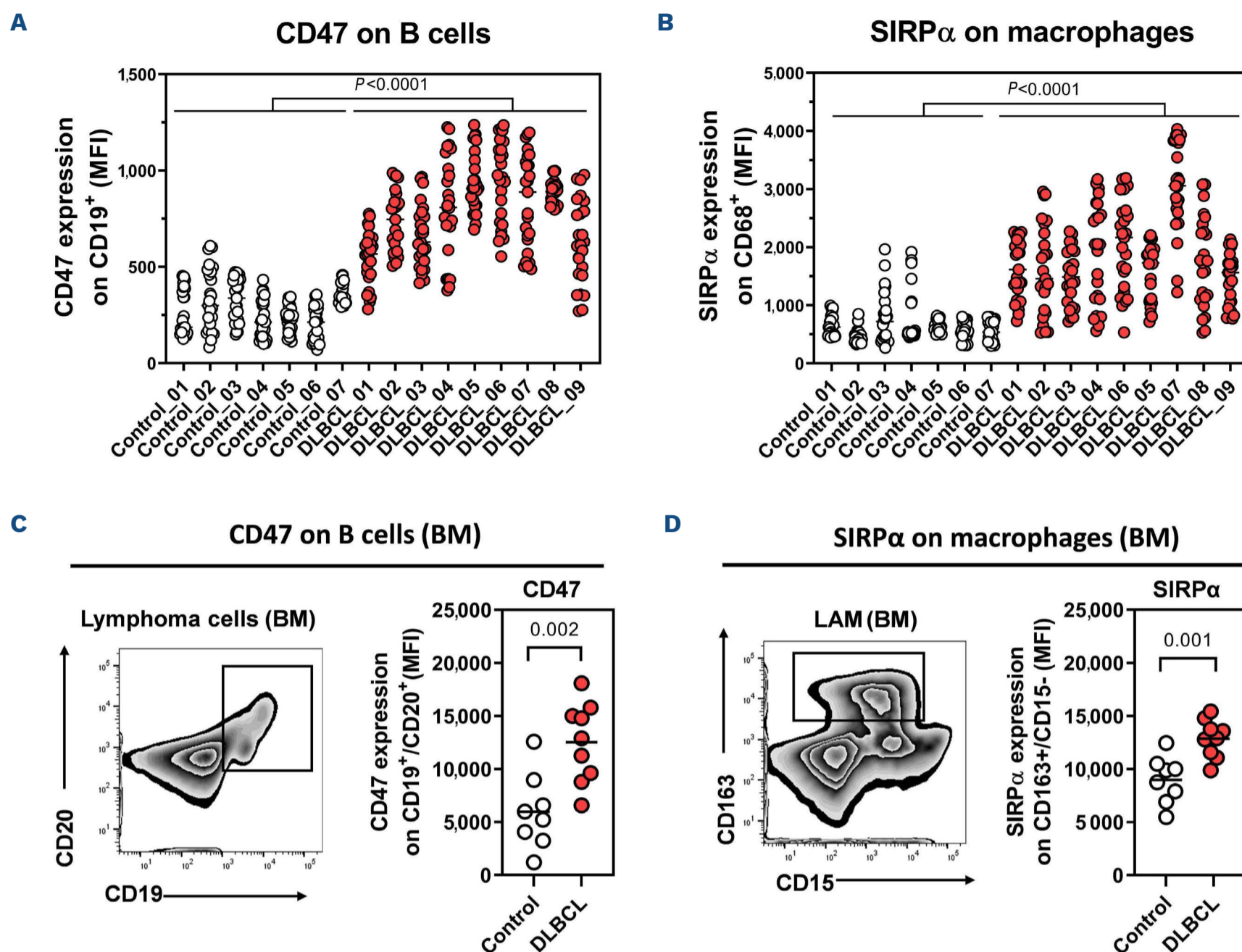


**Figure 1. Increased expression of CD47 and SIRP $\alpha$  in diffuse large B-cell lymphoma.** (A) Expression of CD47 on B cells (CD19<sup>+</sup>) was quantified using confocal microscopy on tonsils as benign controls (white circles) (N=7) or diffuse large B-cell lymphoma (DLBCL) specimens (red circles) (N=9). (B) SIRP $\alpha$  on macrophages (CD68<sup>+</sup>) was quantified using confocal microscopy on tonsils as benign controls (white circles) (N=7) or DLBCL specimens (red circles) (N=9). Regions of interest matching B cells or macrophages were segmented using Zeiss-software (ZEN 2.6) or the open-source software QuPath (<https://qupath.github.io>), and the mean fluorescence intensity of CD47 or SIRP $\alpha$  was assessed for each region of interest. Data for 25 cells from each donor were plotted for CD47 or SIRP $\alpha$ . Lines show the mean value. (C, D) Bone marrow biopsies from healthy controls (N=8, white circles) or DLBCL patients with tumor infiltration (N=9, red circles) were analyzed for (C) the expression of CD47 on B cells/lymphoma cells (CD19<sup>+</sup>/CD20<sup>+</sup>) or (D) SIRP $\alpha$  on macrophages/lymphoma-associated macrophages (CD163<sup>+</sup>/CD15<sup>-</sup>). The graphs (C, D) show the result of five independent experiments. Each dot represents a tested donor. A nonparametric Mann-Whitney U test was performed. Lines show the mean value. MFI: mean fluorescence intensity; BM: bone marrow; LAM: lymphoma-associated macrophages.

timepoint of 3 h, we performed real-time Incucyte<sup>®</sup> analysis to observe phagocytosis over a longer period (Figure 3C). Measured over a time span of 6 h, clearance of lymphoma cells was increased under combined treatment with tafasitamab and anti-CD47 monoclonal antibody compared to the clearance in response to single treatments. Since it cannot be excluded that the anti-CD47 clone (B6H12, mouse IgG1), used in the above experiments, triggers ADCP on its own via engagement of Fc receptors, we used an Fc-modified antibody variant (CD47-IgG $\alpha$ ) with abrogated Fc $\gamma$ R binding as a control.<sup>15</sup> Independent of their Fc domain, both CD47 antibodies significantly increased tafasitamab-mediated

phagocytosis of lymphoma cells (*Online Supplementary Figure S5*), suggesting that enhanced phagocytosis results from blockade of the CD47 signaling pathway.

Next, the effect of combination treatment on primary patients' samples was examined (for the patients' characteristics see *Online Supplementary Table S2*). LAM were isolated from lymph node or bone marrow biopsy samples from newly diagnosed DLBCL patients using FACS and co-cultured with isolated autologous lymphoma cells in the presence or absence of tafasitamab  $\pm$  anti-CD47 monoclonal antibody (Figure 4A, B). LAM isolated from lymph node or bone marrow samples showed similar tafasitamab-mediated phago-

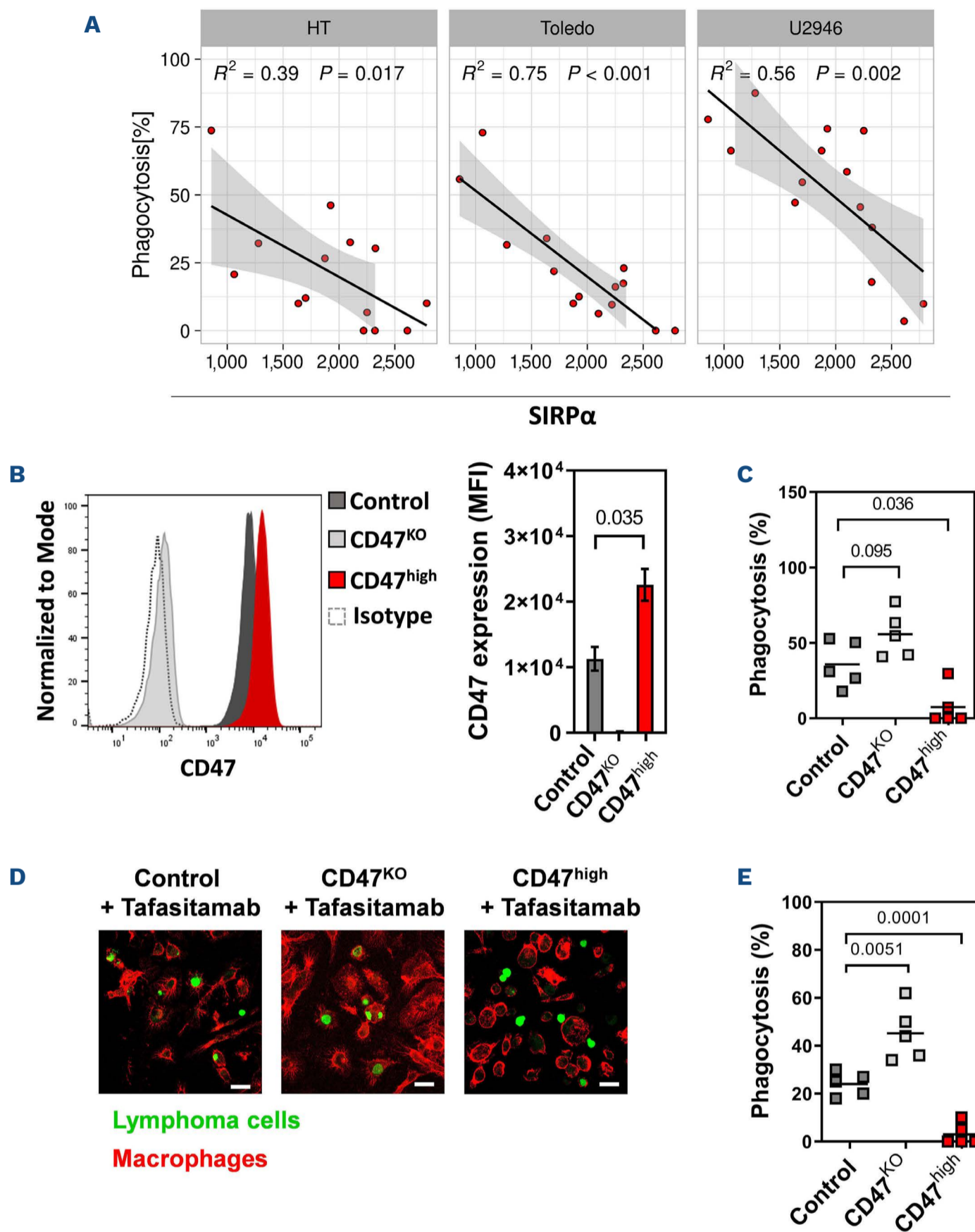


**Figure 2. The CD47-SIRP $\alpha$  axis impairs tafasitamab-mediated phagocytosis.** (A) *In vitro*-differentiated macrophages were analyzed for SIRP $\alpha$  expression by flow cytometry before they were used for assays of antibody-dependent cellular phagocytosis (ADCP) (N=13). Tafasitamab-induced phagocytosis of HT, Toledo and U2946 cell lines was correlated with SIRP $\alpha$  expression on macrophages. A simple linear model was fitted to the data and the  $R^2$  value was calculated. (B) The CRISPR/Cas9 system was used to alter gene expression in Toledo cells. CD47 expression on CD47 knock out (CD47<sup>KO</sup>, light gray), CD47 overexpressing (CD47<sup>high</sup>, red) and wild-type Toledo (control, dark gray) cells, determined by flow cytometry (N=5). The dotted line represents the isotype control. MFI is defined as median fluorescence intensity. The bar chart shows average MFI values of three independent measurements. Error bars show the standard error of the mean. A two-tailed paired Student *t* test was performed. (C) Tafasitamab-mediated phagocytosis of control, CD47<sup>KO</sup> or CD47<sup>high</sup> cells measured by flow cytometry. Lines show the mean value. The graph shows the result of five independent experiments. A two-tailed paired Student *t* test was performed. (D) Immunofluorescence of *in vitro*-differentiated macrophages co-cultured with different cell lines (control, CD47<sup>KO</sup>, CD47<sup>high</sup>) and tafasitamab (1  $\mu$ g/mL) for 3 h. Lymphoma cells lines were stained with Cytolight Rapid Green Dye (green), macrophages were stained with CD11b-APC (red). The microscopy images show representative sections of five experiments. (E) Quantification of phagocytosis of Toledo cells (control, dark gray) and the genetically modified cells (CD47<sup>KO</sup>: light gray; CD47<sup>high</sup>: red) by confocal microscopy. One hundred macrophages per condition were counted and the percentage with ingested lymphoma cells was calculated. The graph shows the result of five independent experiments. A two-tailed paired Student *t* test was performed. Lines show the mean value. Scale bar: 20  $\mu$ m.

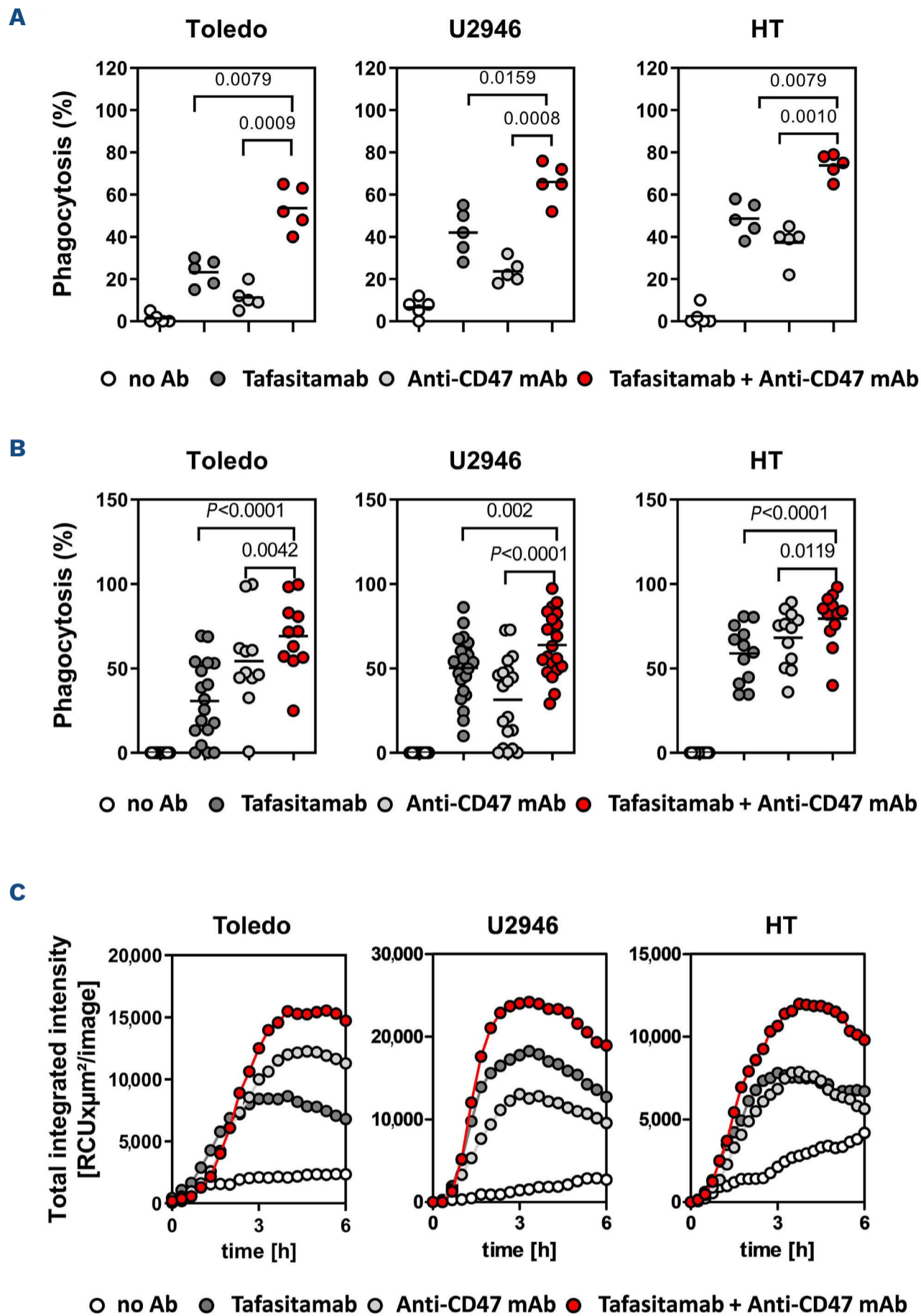


**Figure 3. Blocking CD47 increases tafasitamab-mediated phagocytosis.** (A) For quantification of phagocytosis of different diffuse large B-cell lymphoma (DLBCL) cell lines (Toledo, U2946, HT) by confocal microscopy, 100 macrophages per condition were counted and the percentage with ingested lymphoma cells was calculated. Lines show the mean value. The graphs show the results of five independent experiments. A two-tailed paired Student  $t$  test was performed. (B) Percentage phagocytosis of lymphoma cell lines using *in vitro*-differentiated macrophages as effector cells, in the presence or absence of tafasitamab and anti-CD47 monoclonal antibody. Phagocytosis was measured with flow cytometry. The diagrams show the results of several independent experiments (Toledo: N=11; U2946: N=23; HT: N=12). A two-tailed paired Student  $t$  test was performed. Lines show the mean value. (C) Phagocytosis of lymphoma cell lines in the presence or absence of tafasitamab and/or anti-CD47 monoclonal antibody for 6 h. Incubation and measurements were performed in the absence (white circles) or presence of tafasitamab (dark gray circles) or anti-CD47 (light gray circles) or a combination of both (red circles). Measurements and analysis were conducted using an Incucyte<sup>®</sup> Live Cell Imaging system microscopy and Incucyte<sup>®</sup> 2022A software. Total red signal per image was evaluated for all conditions and timepoints. The course of total red signal is shown in the plots for three cell lines. The graph shows a representative result of three independent experiments. Ab: antibody; mAb: monoclonal antibody; RCU: red mean intensity object average.

cytosis efficiency to *in vitro*-differentiated macrophages. Furthermore, combination treatment with tafasitamab and anti-CD47 resulted in significantly increased phagocytosis of autologous lymphoma cells *ex vivo*, compared to monotherapy (lymph nodes, tafasitamab: 40 $\pm$ 14% vs. tafasitamab + anti-CD47: 60 $\pm$ 12%;  $P=0.002$ ; bone marrow, tafasitamab: 41 $\pm$ 23% vs. tafasitamab + anti-CD47: 60 $\pm$ 28%;  $P=0.05$ ) (Figure 4C). These results suggest that CD47 blockade can improve the phagocytic activity mediated by tafasitamab targeting primary DLBCL patients' cells.

### Combination of tafasitamab and anti-CD47 enhances phagocytosis of CD19<sup>low</sup> lymphoma cells

CD19 expression in lymphoma is very variable and diminished CD19 expression was observed in a substantial percentage of DLBCL patients (24% to 33%) in different studies.<sup>17,18</sup> Thus, we aimed to determine whether CD47 blockade can boost the phagocytic potential of tafasitamab against lymphoma cells with low CD19 expression. To simulate this scenario, we sorted Toledo cells based on their CD19 expression level into high (CD19<sup>high</sup>) and low (CD19<sup>low</sup>) populations (with the MFI of CD19<sup>low</sup> cells being four times lower than that of CD19<sup>high</sup> cells) (Figure 5A, *Online Supplementary Figure S6A*) and co-incubated them with macrophages in the presence or absence of tafasitamab, anti-CD47 or the combination of both. Notably, isolated lymphoma cells showed no significant difference in terms of viability or CD47 expression (*Online Supplementary Figure S6B*) and the difference in CD19 expression was stable for 24 h after sorting. As expected, tafasitamab-mediated phagocytosis of CD19<sup>low</sup> cells was decreased compared with phagocytosis of CD19<sup>high</sup> target cells (CD19<sup>high</sup>: 41 $\pm$ 7% vs. CD19<sup>low</sup>: 15 $\pm$ 9%) (Figure 5B). Treatment with anti-CD47 alone mediated a similar increase in phagocytosis in both CD19<sup>low</sup> and CD19<sup>high</sup> lymphoma cells compared to control samples. Most importantly, combination treatment compared to tafasitamab alone significantly increased phagocytosis of CD19<sup>low</sup> cells, which was in a similar range as the phagocytosis rate of CD19<sup>high</sup> cells (CD19<sup>high</sup>: 56 $\pm$ 7% vs. CD19<sup>low</sup>: 54 $\pm$ 10%). These results could also be verified using confocal microscopy. While ~40% of CD19<sup>high</sup> cells were ingested by macrophages upon tafasitamab treatment, only ~10% of CD19<sup>low</sup> cells were phagocytosed (Figure 5C, D). Consistent with the flow cytometry data, combination treatment with tafasitamab and anti-CD47 induced similar levels of increase in phagocytosis of both CD19<sup>high</sup> and CD19<sup>low</sup> cells when compared to tafasitamab treatment alone. Taken together, these data suggest that addition of anti-CD47 blockade enhances tafasitamab-mediated phagocytic elimination of lymphoma cells with low CD19 expression.

### Combination therapy with tafasitamab and anti-CD47 antibody prolongs animal survival and decelerates tumor growth in mice

To assess the effect of combination treatment with tafasitamab and an anti-CD47 antibody *in vivo*, we used two different

lymphoma xenograft models. First, we used a disseminated Ramos C.B-17 SCID model. SCID mice have functional natural killer (NK) cells mediating ADCC, which is an additional important mode of action of tafasitamab besides ADCP. Ramos cells express high levels of CD47 and CD19 (*Online Supplementary Figure S7*) and are commonly used to assess the *in vivo* performance of antibody therapeutics.<sup>19,20</sup> Between days 5 and 21 after tumor cell inoculation, mice were treated with either vehicle control (PBS), tafasitamab, anti-CD47 antibody (clone B6H12) or the antibody combination (Figure 6A). While control-treated mice reached endpoints after a median of 25 days, animals treated with tafasitamab or anti-CD47 alone showed significantly improved outcomes with a median survival of 35 days or >99 days, respectively (tafasitamab vs. control:  $P<0.0001$ ; anti-CD47 vs. control:  $P<0.0001$ ) (Figure 6B). Combination treatment yielded significantly improved survival compared to the single treatments, as 0/15 tafasitamab-treated, 11/15 anti-CD47-treated and 15/15 combination-treated mice were alive at the end of the study (tafasitamab vs. tafasitamab + anti-CD47:  $P<0.0001$ ; anti-CD47 vs. tafasitamab + anti-CD47:  $P=0.035$ ).

Next, the combination was tested in a flank Ramos xenograft model in NOD/SCID mice. In NOD/SCID mice, NK cell function is partially compromised and binding affinity of murine SIRP $\alpha$  to human CD47 is increased compared to SIRP $\alpha$  from other mouse strains or human SIRP $\alpha$ .<sup>21-23</sup> Treatment with either vehicle control (PBS), tafasitamab, anti-CD47 antibody (clone B6H12) or the antibody combination started on day 6 after tumor cell inoculation and continued for up to 4 weeks (Figure 6C). While tumor growth delay was observed in the tafasitamab- and anti-CD47- monotherapy groups when compared to the vehicle control (2 or 14 days, respectively), the combination outperformed the monotherapies (Figure 6D). Percent survival was determined by the number of animals reaching maximal tumor volume of 1,500 mm<sup>3</sup> until the end of the study (Figure 6E). On day 55, 0/10 control, 0/10 tafasitamab-treated, and 1/10 anti-CD47 antibody-treated animals were still alive, while, 7/10 animals were still alive in the combination treatment group, demonstrating a significant survival benefit of the combination treatment compared to the single treatments (tafasitamab vs. tafasitamab + anti-CD47 monoclonal antibody:  $P<0.0001$ ; anti-CD47 vs. tafasitamab + anti-CD47:  $P=0.0017$ ). In summary, CD47 checkpoint blockade enhances the anti-tumor efficacy of tafasitamab in lymphoma tumor models *in vivo*.

## Discussion

In high-grade B-cell lymphomas such as DLBCL, macrophages represent a key component of the tumor microenvironment and significant sentinels of the antitumor immune response.<sup>24,25</sup> Despite the fact that macrophages are important effector cells for antibody-based therapies, lymphoma cells can manipulate the effector functions of

macrophages via altered expression of proteins<sup>26-28</sup> and counteract their ADCP capacity via the CD47/SIRP $\alpha$  axis.<sup>10</sup> In this study, we show that expression of CD47 and SIRP $\alpha$  is upregulated in primary DLBCL samples. While the studied population of patients in this work was small, a significant increase in CD47 expression was detected in both lymph nodes and tumor-infiltrated bone marrow of DLBCL patients,

which is in line with the findings of previous studies.<sup>29,30</sup> It has also been reported that high CD47 mRNA expression is associated with a poorer clinical prognosis in DLBCL, B-chronic lymphocytic leukemia and mantle cell lymphoma and a higher risk of death in DLBCL patients.<sup>10,31</sup> Moreover, we found that primary human LAM from DLBCL patients exhibited increased expression of the CD47 interaction

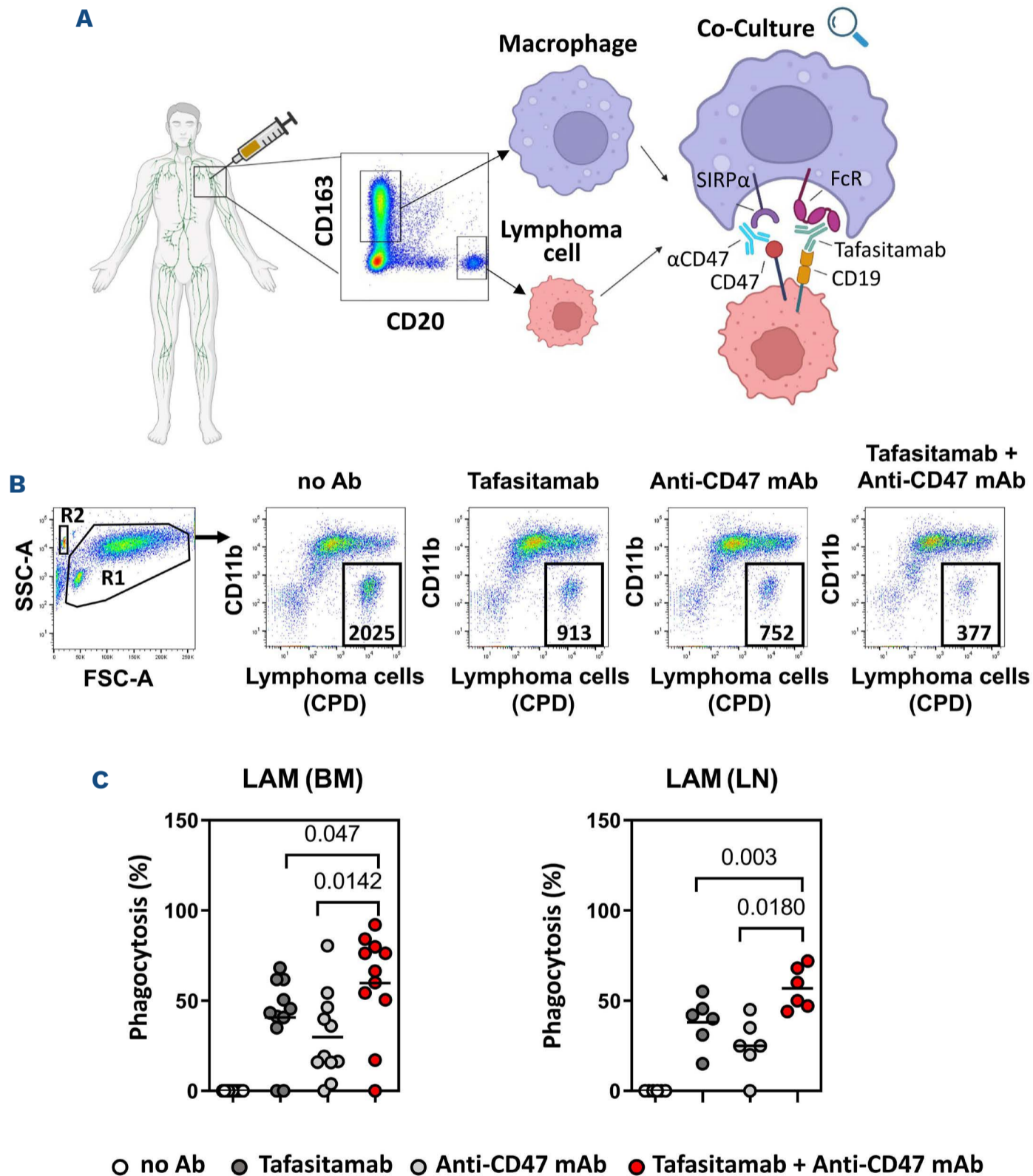


**Figure 4. Blockade of CD47 enhances tafasitamab-mediated phagocytosis of lymphoma-associated macrophages.** (A) Schematic illustration of flow cytometric isolation of lymphoma-associated macrophages (LAM) and primary lymphoma cells from bone marrow (BM) (N=11) and lymph nodes (LN) (N=6) of patients with diffuse large B-cell lymphoma (DLBCL). (B) Representative gating strategy and fluorescence activated cell sorting plots for determination of phagocytosis. Isolated lymphoma cells were stained with CPD and co-cultured with isolated LAM (gate R1). Macrophage effector cells were counterstained with an anti-CD11b antibody and absolute numbers of remaining CD11b<sup>-</sup>/CPD<sup>+</sup> lymphoma cells were determined using counting beads (gate R2). (C) Phagocytosis of primary lymphoma cells by LAM isolated from DLBCL patients' BM (left graph) or LN (right graph), in the presence or absence of tafasitamab and anti-CD47 monoclonal antibody. Phagocytosis was measured by flow cytometry. The graphs show the results of several independent experiments (LAM BM: N=11; LAM LN: N=6). A two-tailed paired Student *t* test was performed. Lines show the mean value. SSC: side scatter; FSC: forward scatter; Ab: antibody; mAb: monoclonal antibody.



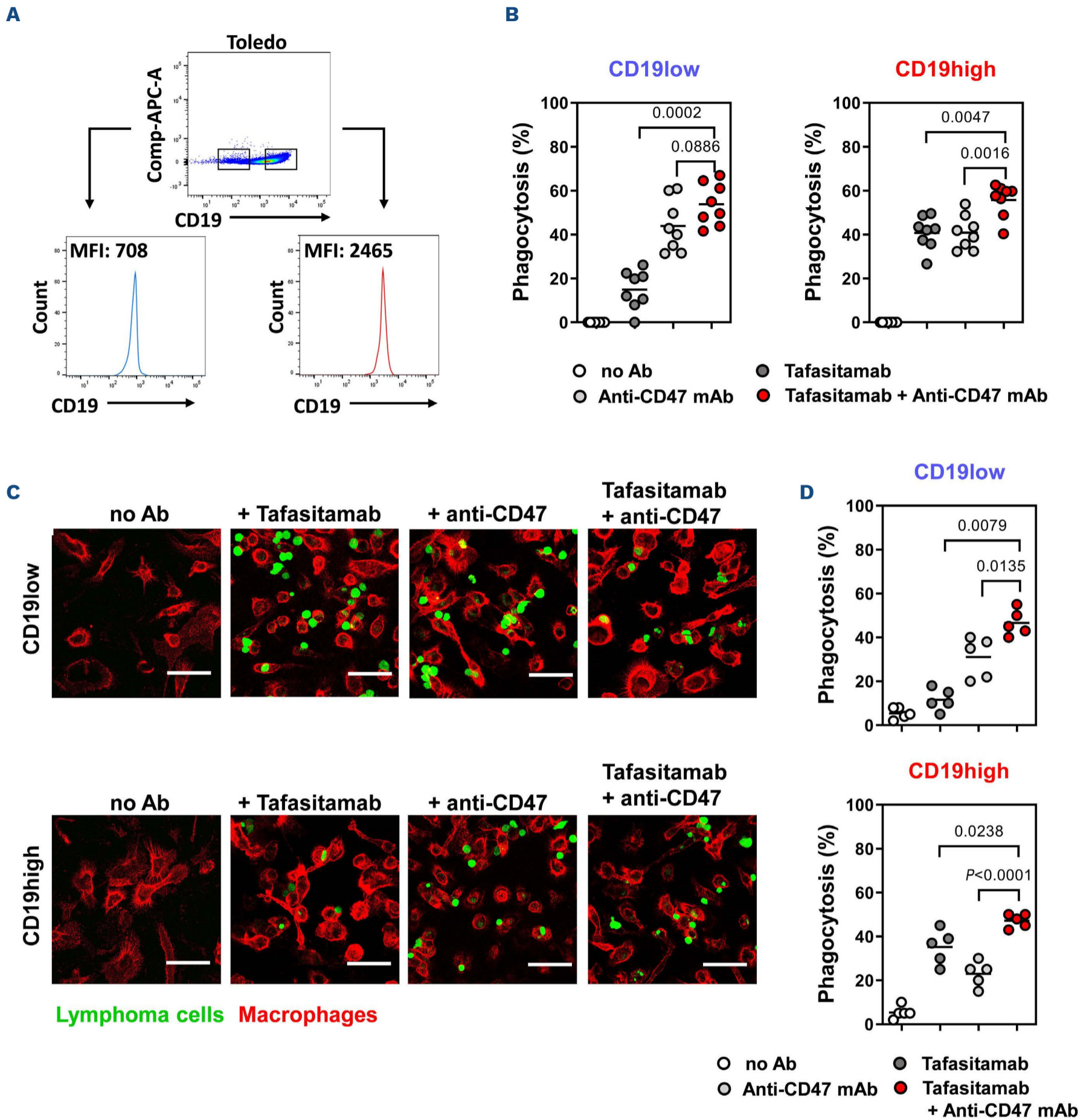


**Figure 5. A combination of tafasitamab and anti-CD47 increases the elimination of CD19<sup>low</sup>-expressing lymphoma cells.** (A) CD19<sup>low</sup> (blue histogram) or CD19<sup>high</sup> (red histogram) Toledo cells were isolated by flow activated cytometric cell sorting (FACS). (B, C) Sorted cell populations were immediately incubated with *in vitro*-differentiated macrophages and phagocytosis in the presence or absence of tafasitamab and/or anti-CD47 was determined after 3 h by flow cytometry (B) or confocal microscopy (C). The graphs in (B) summarize the results of eight macrophage donors tested by FACS in eight independent experiments. A two-tailed paired Student *t* test was performed. Lines show the mean value. (C) CD19<sup>low</sup> and CD19<sup>high</sup> Toledo cells were stained with Cytolight Rapid Green Dye (green), macrophages were stained with CD11b-APC (red) and phagocytosis was analyzed by confocal microscopy. Images were taken after washing steps, removing non-adherent and/or non-phagocytosed cells. The microscopy images show representative sections of five experiments performed. Scale bar: 20  $\mu$ m. (D) For quantification of phagocytosis of sorted CD19<sup>low</sup> (upper panel) or CD19<sup>high</sup> (lower panel) Toledo cells by confocal microscopy, 100 macrophages per condition were counted and the percentage with ingested lymphoma cells was calculated. The graphs show the result of five independent experiments. A two-tailed paired Student *t* test was performed. Lines show the mean value. MFI: mean fluorescence intensity; Ab: antibody; mAb: monoclonal antibody;

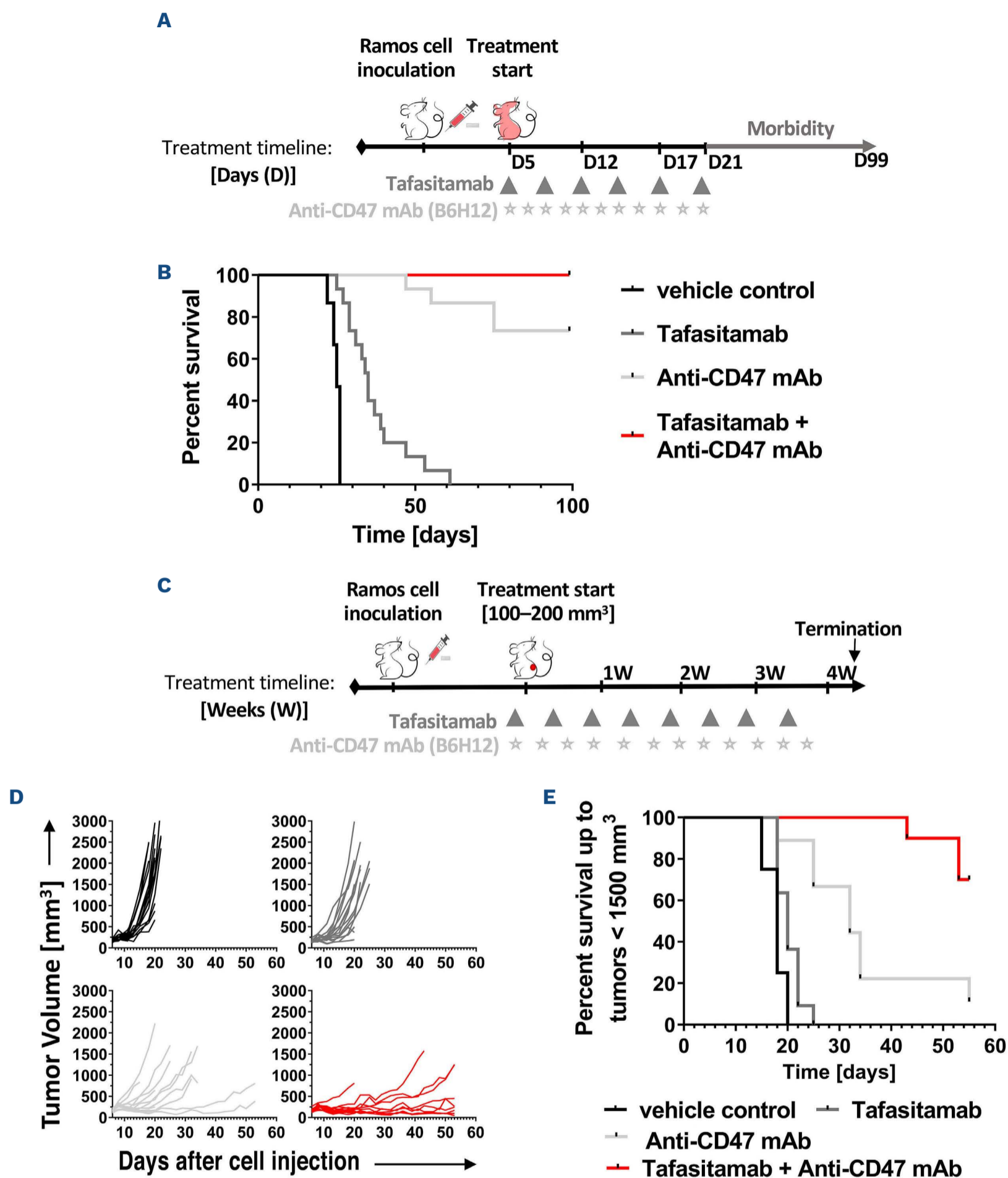


**Figure 6. Combination treatment with tafasitamab and anti-CD47 antibody prolongs survival and decelerates tumor growth in mice.** (A) Schematic illustration of the disseminated xenograft model. Ramos cells were injected intravenously on day 0. Treatment with tafasitamab, anti-CD47 (clone B6H12) and the combination commenced on day 5 and was continued until day 21, followed by continuous monitoring of animals for signs of morbidity until day 99. (B) Kaplan–Meier plot of the disseminated survival model following treatment with tafasitamab, CD47 monoclonal antibody or the combination. Tafasitamab vs. control:  $P < 0.0001$ , anti-CD47 vs. control:  $P < 0.0001$ , tafasitamab vs. tafasitamab + anti-CD47:  $P < 0.0001$ , anti-CD47 vs. tafasitamab + anti-CD47:  $P = 0.035$ . (C) Schematic illustration of the flank xenograft model. Ramos cells were injected subcutaneously into the right flank of each mouse on day 0. Treatment with tafasitamab, anti-CD47 (clone B6H12) monoclonal antibody was started and continued for up to 4 weeks; the study terminated on day 55. (D) Spider plots showing tumor growth curves for individual animals ( $N = 15$ ) for each treatment group. (E) Kaplan–Meier plot showing animal survival until a final tumor volume of 1,500 mm<sup>3</sup> was reached. Tafasitamab vs. control:  $P = 0.0095$ , anti-CD47 vs. control:  $P < 0.0001$ , tafasitamab vs. tafasitamab + anti-CD47 monoclonal antibody:  $P < 0.0001$ ; anti-CD47 vs. tafasitamab + anti-CD47:  $P = 0.0017$ .

partner SIRP $\alpha$ . Interestingly, a correlation of high SIRP $\alpha$  gene expression with a favorable survival of patients treated with R-CHOP was reported for DLBCL,<sup>31</sup> while high SIRP $\alpha$  expression on LAM was reported to correlate with poorer survival in patients with follicular lymphoma.<sup>32</sup> In addition, patients with follicular lymphoma who relapsed or progressed after frontline lenalidomide and rituximab (R<sup>2</sup>) treatment, displayed an increased percentage of SIRP $\alpha$ -positive LAM,<sup>12</sup> which may suggest that this is a mechanism of resistance to R<sup>2</sup> in these patients.

It is unclear why LAM exhibit increased SIRP $\alpha$  expression in comparison to non-malignant controls. While CD47 expression is regulated by the MYC oncogene<sup>33</sup> and cytokines such as interleukin-4,<sup>34</sup> not much is known about the regulation of SIRP $\alpha$ . However, a recent study showed that SIRP $\alpha$  expression in tumor-associated macrophages is transcriptionally repressed by the cyclin-dependent kinase inhibitor CDKN1A (p21).<sup>35</sup> Thus, it would be interesting to clarify in future studies whether p21 or other factors are also responsible for the high SIRP $\alpha$  expression in DLBCL-associated macrophages. Using cell line models, we demonstrated that the CD47/SIRP $\alpha$  axis can negatively affect phagocytic activity mediated by the CD19-targeting antibody tafasitamab. In line with this, phagocytosis was significantly reduced upon overexpression of CD47 in lymphoma cells, suggesting that lymphomas with particularly high CD47 expression may be resistant to tafasitamab-mediated phagocytosis. Furthermore, we found that combining tafasitamab with an anti-CD47 blocking antibody can enhance tafasitamab-mediated phagocytosis using co-cultures of lymphoma cell lines and *in vitro*-differentiated macrophages from healthy donors.

Notably, an Fc-modified antibody variant with abrogated Fc $\gamma$ R binding (CD47-IgG $\sigma$ ), which did not result in notable phagocytosis when applied alone, was also able to increase tafasitamab-mediated phagocytosis, indicating that blocking the CD47/SIRP $\alpha$  axis to decrease the CD47 “don’t eat me” signal is sufficient to achieve a combination benefit together with tafasitamab. The combination of the Fc-silent CD47-IgG $\sigma$  with rituximab previously also led to enhanced ADCP compared to rituximab alone.<sup>15</sup> Recently, Wang *et al.* reported that a SIRP $\alpha$  variant fused to an Fc with inactivated effector function (nFD164) in combination with the anti-CD20 antibody rituximab showed a synergistic antitumor effect in a lymphoma xenograft mouse model, suggesting a concordant conclusion.<sup>36</sup> A more recent study by Osario *et al.* however suggests that anti-CD47 antibodies require both blockade of the CD47/SIRP $\alpha$  axis and engagement of activating Fc $\gamma$ R signaling to achieve significant *in vivo* antitumor activity.<sup>37</sup> More importantly, the findings that the combination of tafasitamab with an Fc-competent anti-CD47 resulted in increased phagocytosis could be confirmed testing primary lymphoma cells and LAM *ex vivo* in an autologous setting. This is of particular importance, as these effector cells represent up to 50% of the total leukocyte content in lymphomas<sup>24,38</sup> and have the potential to rapidly eradicate lymphoma cells

by phagocytosis.<sup>9</sup> Similar combination benefits as seen for the CD19-targeting antibody tafasitamab in combination with CD47 blockade were observed for the CD20-targeting antibody rituximab in combination with CD47 blockade in experiments with cell lines and macrophages from healthy donors as well as primary lymphoma cells and LAM.<sup>10,15</sup> Our study mainly focused on CD47 blockade with a CD47-targeting antibody in the context of macrophages. In recent years, several reports indicated that other immune cells, including T cells and even NK cells, might also be affected by blocking the CD47/SIRP $\alpha$  axis.<sup>39-42</sup> As the CD47/SIRP $\alpha$  axis contributes to bridging innate and adaptive immunity, it would be interesting to take this interplay into account in future studies with tafasitamab – especially as ADCC is one of its major modes of action. In DLBCL, CD19 loss or downregulation after CD19-directed therapies such as CART19 treatment is observed.<sup>43,44</sup> Moreover, CD19 expression in lymphoma is characterized by high variability.<sup>18</sup> Here, we show that Toledo cells with low CD19 expression are as efficiently phagocytosed by macrophages as Toledo cells with high CD19 expression through the combination of tafasitamab and anti-CD47. This observation implies that combination therapy targeting CD19 and CD47 could overcome reduced ADCP efficiency of therapies targeting only CD19 in CD19<sup>low</sup>-expressing cells.

Finally, the combination of tafasitamab and the anti-CD47 clone B6H12 was tested in two different *in vivo* models engrafted with Ramos cells. Our focus here was to reflect different modes of action including not only ADCP, but also ADCC when examining the benefit of the combination of both antibodies *in vivo*, wherefore SCID mice containing functional NK cells were selected as one model. NOD/SCID mice were used as the second model since this model allows good subcutaneous tumor engraftment, although it does have some limitations: compromised NK cells, which likely result in an underestimation of tafasitamab’s ADCC capacity as well as increased binding affinity of NOD murine SIRP $\alpha$  to human CD47 associated with potentially artificially high antitumor effects of anti-CD47 molecules compared to those with other mouse strains.<sup>21-23</sup> Importantly, both approaches significantly improved the survival rates of mice compared to animals treated with the respective single treatments. In the past, Chao *et al.* documented similar benefits from combination treatment with rituximab and an anti-CD47 in both disseminated as well as localized Raji xenograft mouse models.<sup>10</sup> More recently, Dheilly *et al.* generated a dual-targeting bispecific antibody blocking CD47 and CD19 and reported that treatment with the anti-CD47/CD19 bispecific antibody induced significant tumor regression compared to treatment with either anti-CD47 or anti-CD19 antibody in a Raji mouse model.<sup>45</sup> In this model, the combination of anti-CD47 and anti-CD19 antibodies resulted in a similar reduction of tumor volume as the bispecific antibody, confirming the potent antitumor activity upon combination of CD47 blockade with CD19-targeting. Most recently, a fusion protein of a CD20 antibody with the CD47 binding domain of SIRP $\alpha$  was shown

to reduce tumor size and activate both macrophages and NK cells via blockade of the CD47/SIRP $\alpha$  interaction and Fc $\gamma$ R engagement in different mouse xenograft tumor models.<sup>46</sup> In summary, numerous approaches combining targeting of B-cell surface proteins such as CD19 or CD20 and the CD47/SIRP $\alpha$  axis in different molecule formats are currently under investigation and it remains to be elucidated in the future which antigen and format combination will display the best antitumor and fewest side effects in lymphoma treatment.<sup>47</sup> In conclusion, the results presented in this study confirm the relevance of the CD47/SIRP $\alpha$  axis in DLBCL and demonstrate that CD47 blockade with a CD47-targeting antibody enhances the phagocytic and antitumor activity of the CD19-targeted antibody tafasitamab *in vitro* and *in vivo*. Whether combinations of tafasitamab with other compounds inhibiting the CD47/SIRP $\alpha$  pathway are beneficial is currently being investigated in a phase I/IIb trial assessing the safety, tolerability and potential clinical benefits of the CD47-targeting SIRP $\alpha$  fusion protein maplirpacept (TTI-662) in combination with tafasitamab and lenalidomide in relapsed/refractory DLBCL patients (NCT05626322).

### Disclosures

MP-K, DME, CA, KIB, and SS are employees of Morphosys AG. SS owns MorphoSys stocks. MP and SS hold MorphoSys patents. This study received funding from MorphoSys AG. The funder was involved in the study design, collection, analysis, interpretation of the data, writing of this article and decision to submit it for publication.

### Contributions

AB designed and performed experiments and helped to write

the manuscript. MP-K and DM conceived the project, designed experiments and helped to write the manuscript. MB-H and SB selected and evaluated histopathological lymphoma specimens and controls and established the immunohistochemical staining. DM-E designed and supervised animal experiments. JB designed and performed experiments. CK and AL contributed essential reagents/analytical tools and scientific input. CA designed experiments. KI-B designed experiments and helped to write the manuscript. SH, CL, and JV performed the statistical analysis. SA, JB, SV, FB, and BJ provided patients' materials and provided critical suggestions and discussions throughout the study. SS helped to write the manuscript. AM provided major intellectual input for the project design and helped to write the manuscript. HB conceived and directed the project and wrote the manuscript.

### Acknowledgments

We would like to acknowledge the excellent assistance of the Core Unit Cell Sorting and Immunomonitoring Erlangen.

### Funding

HB was supported by the Wilhelm-Sander Foundation, by the Research Training Group 2740 "Immunomicrotope" (project B3), by the German Cancer Foundation (grant n. 70114489) and by the SFB TR 221 (project B12). MB-H was supported by the SFB TR 221 (project Z01). AL was supported by the Research Training Group 2740 "Immunomicrotope" (project A3).

### Data-sharing statement

The original contributions presented in the study are included in the article or Online Supplementary Material. Further inquiries can be directed to the corresponding author.

## References

- Alaggio R, Amador C, Anagnostopoulos I, et al. The 5th edition of the World Health Organization classification of haematolymphoid tumours: lymphoid neoplasms. *Leukemia*. 2022;36(7):1720-1748.
- Crump M, Neelapu SS, Farooq U, et al. Outcomes in refractory diffuse large B-cell lymphoma: results from the international SCHOLAR-1 study. *Blood*. 2017;130(16):1800-1808.
- Pfreundschuh M, Kuhnt E, Trumper L, et al. CHOP-like chemotherapy with or without rituximab in young patients with good-prognosis diffuse large-B-cell lymphoma: 6-year results of an open-label randomised study of the MabThera International Trial (MINT) Group. *Lancet Oncol*. 2011;12(11):1013-1022.
- Her JH, Pretscher D, Patra-Kneuer M, et al. Tafasitamab mediates killing of B-cell non-Hodgkin's lymphoma in combination with gammadelta T cell or allogeneic NK cell therapy. *Cancer Immunol Immunother*. 2022;71(11):2829-2836.
- Horton HM, Bennett MJ, Pong E, et al. Potent *in vitro* and *in vivo* activity of an Fc-engineered anti-CD19 monoclonal antibody against lymphoma and leukemia. *Cancer Res*. 2008;68(19):8049-8057.
- Uchida J, Hamaguchi Y, Oliver JA, et al. The innate mononuclear phagocyte network depletes B lymphocytes through Fc receptor-dependent mechanisms during anti-CD20 antibody immunotherapy. *J Exp Med*. 2004;199(12):1659-1669.
- Kridel R, Steidl C, Gascoyne RD. Tumor-associated macrophages in diffuse large B-cell lymphoma. *Haematologica*. 2015;100(2):143-145.
- Hermann M, Niemitz C, Marafioti T, Schriever F. Reduced phagocytosis of apoptotic cells in malignant lymphoma. *Int J Cancer*. 1998;75(5):675-679.
- Bruns H, Buttner M, Fabri M, et al. Vitamin D-dependent induction of cathelicidin in human macrophages results in cytotoxicity against high-grade B cell lymphoma. *Sci Transl Med*. 2015;7(282):282ra47.
- Chao MP, Alizadeh AA, Tang C, et al. Anti-CD47 antibody synergizes with rituximab to promote phagocytosis and eradicate non-Hodgkin lymphoma. *Cell*. 2010;142(5):699-713.
- Seiffert M, Cant C, Chen Z, et al. Human signal-regulatory protein is expressed on normal, but not on subsets of leukemic myeloid cells and mediates cellular adhesion involving its counterreceptor CD47. *Blood*. 1999;94(11):3633-3643.

12. Marques-Piubelli ML, Parra ER, Feng L, et al. SIRP $\alpha$ + macrophages are increased in patients with FL who progress or relapse after frontline lenalidomide and rituximab. *Blood Adv.* 2022;6(11):3286–3293.
13. Petrova PS, Viller NN, Wong M, et al. TTI-621 (SIRP $\alpha$ Fc): a CD47-blocking innate immune checkpoint inhibitor with broad antitumor activity and minimal erythrocyte binding. *Clin Cancer Res.* 2017;23(4):1068–1079.
14. Advani R, Flinn I, Popplewell L, et al. CD47 blockade by Hu5F9-G4 and rituximab in non-Hodgkin's lymphoma. *N Engl J Med.* 2018;379(18):1711–1721.
15. Zeller T, Lutz S, Munnich IA, et al. Dual checkpoint blockade of CD47 and LILRB1 enhances CD20 antibody-dependent phagocytosis of lymphoma cells by macrophages. *Front Immunol.* 2022;13:929339.
16. Busch L, Mougiakakos D, Buttner-Herold M, et al. Lenalidomide enhances MOR202-dependent macrophage-mediated effector functions via the vitamin D pathway. *Leukemia.* 2018;32(11):2445–2458.
17. Schuster SJ, Bishop MR, Tam CS, et al. Tisagenlecleucel in adult relapsed or refractory diffuse large B-cell lymphoma. *N Engl J Med.* 2019;380(1):45–56.
18. Yang W, Agrawal N, Patel J, et al. Diminished expression of CD19 in B-cell lymphomas. *Cytometry B Clin Cytom.* 2005;63(1):28–35.
19. Schliemann C, Palumbo A, Zuberbuhler K, et al. Complete eradication of human B-cell lymphoma xenografts using rituximab in combination with the immunocytokine L19-IL2. *Blood.* 2009;113(10):2275–2283.
20. Daniel D, Yang B, Lawrence DA, et al. Cooperation of the proapoptotic receptor agonist rhApo2L/TRAIL with the CD20 antibody rituximab against non-Hodgkin lymphoma xenografts. *Blood.* 2007;110(12):4037–4046.
21. Miao M, Masengere H, Yu G, Shan F. Reevaluation of NOD/SCID mice as NK cell-deficient models. *Biomed Res Int.* 2021;2021:8851986.
22. Kwong LS, Brown MH, Barclay AN, Hatherley D. Signal-regulatory protein alpha from the NOD mouse binds human CD47 with an exceptionally high affinity-- implications for engraftment of human cells. *Immunology.* 2014;143(1):61–67.
23. Iwamoto C, Takenaka K, Urata S, et al. The BALB/c-specific polymorphic SIRP $\alpha$  enhances its affinity for human CD47, inhibiting phagocytosis against human cells to promote xenogeneic engraftment. *Exp Hematol.* 2014;42(3):163–171.
24. Gentles AJ, Newman AM, Liu CL, et al. The prognostic landscape of genes and infiltrating immune cells across human cancers. *Nat Med.* 2015;21(8):938–945.
25. Mantovani A, Allavena P, Marchesi F, Garlanda C. Macrophages as tools and targets in cancer therapy. *Nat Rev Drug Discov.* 2022;21(11):799–820.
26. Dahal LN, Dou L, Hussain K, et al. STING activation reverses lymphoma-mediated resistance to antibody immunotherapy. *Cancer Res.* 2017;77(13):3619–3631.
27. Izquierdo E, Vorholt D, Blakemore S, et al. Extracellular vesicles and PD-L1 suppress macrophages, inducing therapy resistance in TP53-deficient B-cell malignancies. *Blood.* 2022;139(25):3617–3629.
28. Su S, Zhao J, Xing Y, et al. Immune checkpoint inhibition overcomes ADCP-Induced immunosuppression by macrophages. *Cell.* 2018;175(2):442–457.e423.
29. Bouwstra R, He Y, de Boer J, et al. CD47 expression defines efficacy of rituximab with CHOP in non-germinal center B-cell (non-GCB) diffuse large B-cell lymphoma patients (DLBCL), but not in GCB DLBCL. *Cancer Immunol Res.* 2019;7(10):1663–1671.
30. Cho J, Yoon SE, Kim SJ, Ko YH, Kim WS. CD47 overexpression is common in intestinal non-GCB type diffuse large B-cell lymphoma and associated with 18q21 gain. *Blood Adv.* 2022;6(24):6120–6130.
31. Carreras J, Kikuti YY, Miyaoka M, et al. Integrative statistics, machine learning and artificial intelligence neural network analysis correlated CSF1R with the prognosis of diffuse large B-cell lymphoma. *Hemato.* 2021;2(2):182–206.
32. Chen YP, Kim HJ, Wu H, et al. SIRP $\alpha$  expression delineates subsets of intratumoral monocyte/macrophages with different functional and prognostic impact in follicular lymphoma. *Blood Cancer J.* 2019;9(10):84.
33. Casey SC, Tong L, Li Y, et al. MYC regulates the antitumor immune response through CD47 and PD-L1. *Science.* 2016;352(6282):227–231.
34. Pena-Martinez P, Ramakrishnan R, Hogberg C, Jansson C, Nord DG, Jaras M. Interleukin 4 promotes phagocytosis of murine leukemia cells counteracted by CD47 upregulation. *Haematologica.* 2022;107(4):816–824.
35. Allouch A, Voisin L, Zhang Y, et al. CDKN1A is a target for phagocytosis-mediated cellular immunotherapy in acute leukemia. *Nat Commun.* 2022;13(1):6739.
36. Wang Z, Hu N, Wang H, et al. High-affinity decoy protein, nFD164, with an inactive Fc region as a potential therapeutic drug targeting CD47. *Biomed Pharmacother.* 2023;162:114618.
37. Osorio JC, Smith P, Knorr DA, Ravetch JV. The antitumor activities of anti-CD47 antibodies require Fc-Fc $\gamma$ R interactions. *Cancer Cell.* 2023;41(12):2051–2065.
38. Newman AM, Liu CL, Green MR, et al. Robust enumeration of cell subsets from tissue expression profiles. *Nat Methods.* 2015;12(5):453–457.
39. Liu X, Pu Y, Cron K, et al. CD47 blockade triggers T cell-mediated destruction of immunogenic tumors. *Nat Med.* 2015;21(10):1209–1215.
40. Nath PR, Gangaplara A, Pal-Nath D, et al. CD47 expression in natural killer cells regulates homeostasis and modulates immune response to lymphocytic choriomeningitis virus. *Front Immunol.* 2018;9:2985.
41. Deuse T, Hu X, Agbor-Enoh S, et al. The SIRP $\alpha$ -CD47 immune checkpoint in NK cells. *J Exp Med.* 2021;218(3):e20200839.
42. van Duijn A, Van der Burg SH, Scheeren FA. CD47/SIRP $\alpha$  axis: bridging innate and adaptive immunity. *J Immunother Cancer.* 2022;10(7):e004589.
43. Yu H, Sotillo E, Harrington C, et al. Repeated loss of target surface antigen after immunotherapy in primary mediastinal large B cell lymphoma. *Am J Hematol.* 2017;92(1):E11–E13.
44. Shalabi H, Kraft IL, Wang HW, et al. Sequential loss of tumor surface antigens following chimeric antigen receptor T-cell therapies in diffuse large B-cell lymphoma. *Haematologica.* 2018;103(5):e215–e218.
45. Dheilly E, Moine V, Broyer L, et al. Selective blockade of the ubiquitous checkpoint receptor CD47 is enabled by dual-targeting bispecific antibodies. *Mol Ther.* 2017;25(2):523–533.
46. Yu J, Li S, Chen D, et al. IMM0306, a fusion protein of CD20 mAb with the CD47 binding domain of SIRP $\alpha$ , exerts excellent cancer killing efficacy by activating both macrophages and NK cells via blockade of CD47-SIRP $\alpha$  interaction and Fc $\gamma$ R engagement by simultaneously binding to CD47 and CD20 of B cells. *Leukemia.* 2023;37(3):695–698.
47. Yang H, Xun Y, You H. The landscape overview of CD47-based immunotherapy for hematological malignancies. *Biomark Res.* 2023;11(1):15.